

Investigation of the segmented chip forming in High Speed Cutting Processes

Paper: 2001-75

Arno Behrens, Bert Westhoff, Karsten Kalisch

Institute of Design and Production Engineering, Laboratory of Production Engineering,

University of the Federal Armed Forces Hamburg,

Holstenhofweg 85, 22043 Hamburg, Germany.

Phone: ++49 (0) 40 / 6541 – 3342, email: karsten.kalisch@unibw-hamburg.de

Abstract

For the efficient use of modern processing technologies and the expansion of their potentials in improving surface quality, material properties as well as process reliability and economic efficiency (e.g. precision machining, high speed cutting HSC), the understanding of complex chip forming processes takes an important position.

In the modeling of the orthogonal cutting process causes, problems arise as the formulation of suitable separation criteria, the description of the chip segmentation process and the determination of suitable material parameters for extremely high deformation strain rates. As there exists no universal mathematical description for the chip forming process itself, methods of resolution and their implementation into the FE-Software MSC.AutoForge are given in this article.

1 Introduction

The process conditions and process limitations are mainly influenced by the chip forming process in metal cutting manufacturing. The distribution of cutting forces and temperatures, as well as tool wearing, are the consequences of the chip forming. Moreover, the quality of the resulting surface is directly related to the kind of chip formed throughout the process. Some of the characteristic properties of the chip forming process are high local deformation ratios with simultaneous high temperatures and deformation strains. The ascertainment of experimental parameters is limited due to the extreme conditions in the chip forming zone, for example, the temperature distribution in the chip or at the contact surface of the tool cannot be determined with sufficient accuracy.

For these reasons, the chip forming process has been the object of intensive research activities for some time now. Not long since analytical models of the orthogonal cutting process were developed, they were limited by the complexity and the non linearity of the chip formation. The finite element method (FEM) is therefore a good basis for the investigation of the complex chip formation processes and the verification of experimental data. Moreover, the FE-simulation delivers interesting results such as the material flow or the distribution of stresses in the chip, that cannot yet be determined by experiments.

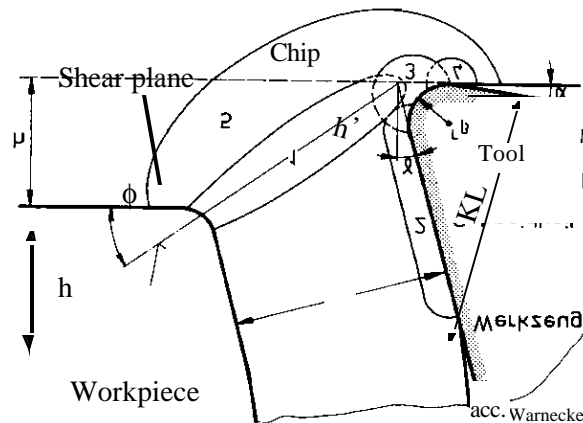


Figure 1 Operating zones in the orthogonal cutting process

Figure 1 shows the chip formation zones of the orthogonal cutting process. Zone 1 is called the primary shear zone where plastic deformation mainly comes from shear yielding of the material in direction of the shear plane. The chip is subjected to an additional shearing strain resulting from high shear friction stresses due to contact with the tool in the secondary shear zone (zone 2).

Directly in front of the cutting edge is zone 3, where the material separation is induced. Zone 4 is characterized by the transition from the cutting edge to the tool flank of the tool. Here

friction occurs between the tool and the new surface of the workpiece. A further influence on the rim zone of the forming process is caused by a pre-travel deformation zone (zone 5)[9].

In most of the materials machined by high speed cutting (HSC) processes, a segmentation of the chip is induced, due to the quasi-adiabatic state in the primary shear zone. First the related problems in model definition are discussed, then a model with the implemented solution strategy is proposed. The experimental results of a real orthogonal cutting process serve as input quantities for this model. The phenomenological evaluation of the resulting chip segments focuses on the primary shear zone as it has the most significant influence on the cutting force. Finally the process relevant values of temperature and stress distribution are evaluated.

2 Material separation

The most significant problem in the simulation of the chip geometry is the modelling of the chip formation process. One of the possibilities consists of the assumption of an ideal-ductile material behavior, thus fully neglecting material separation at all. The metal cutting process is modeled as a forming operation only, where the chip formation is described by a surface enlargement from a continuum mechanics point of view. On the other hand it is possible to model the material separation directly in front of the cutting edge. Then a new workpiece surface is formed from the inside of the material which then comes into contact with the tool flank.

This kind of separation model uses the separation algorithm in [3], which is based on a contact separation of the chip volume. In order to focus on the chip forming process, the tool surface is represented by a line segment. In a simplified view, the tool is defined to be rigid with constant thermal conductivity and infinite elasticity modulus. The cutting edge of the tool has an additional radius which intersects the ground segment as shown in Figure 2.

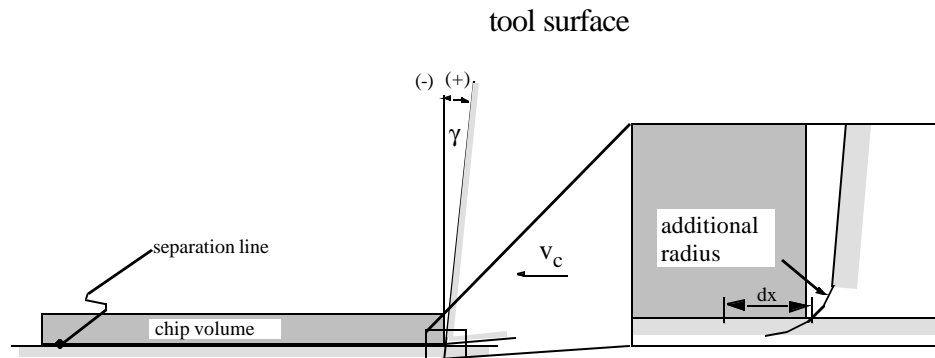


Figure 2 Model of the material separation

This causes a predefined transition of the nodes of the FE-mesh from the ground segment to the cutting edge which is necessary in case of negative cutting angles $\gamma \leq 0^\circ$. The node

separation and the unproblematic transition of the nodes to the tool is obstructed by the forces of pressure in front of the cutting edge. In the case of positive effective cutting angles, this artifice is not necessary. The geometric separation criterion is based on the distance dx between the intersection additional radius / base line and the node in front of the cutting edge. The criterion was integrated by a user subroutine into the FE-simulation.

3 Remeshing

The elements of the shear zone and the off-running chip are subject to a high deformation during the FE-simulation. Moreover, the model ought to consider a discontinuously lamellar chip forming, which coincides with an extreme shear localization in the primary shear zone. An adiabatic shear band formation is often assumed to be the reason for this behavior [4]. Thermal-mechanical instabilities cause a concentration of the material deformation in the shear bands. Locally concentrated high deformation strains, deformation ratios and temperatures with high gradients to the surrounding material are the consequences ([2],[5]). The resulting shear band normally has a width of only some micrometers.

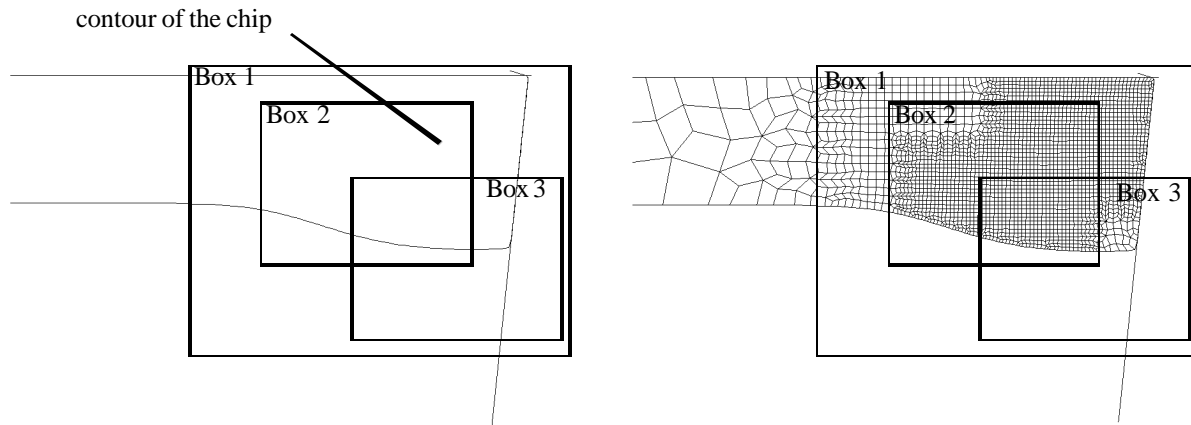


Figure 3 Example of the functionality of the moving boxes

A very fine FE-mesh is necessary in the shear region in order to map the shear band formation and the related local deformation with sufficient accuracy [6]. This has been verified by FE-simulations for the modeling of shear band concentrations. The locally concentrated high gradients of temperature and shear velocities in the shear band region cannot be calculated with sufficient precision in case of wide FE-meshes. The resulting smoothing of the values prevent an exact prediction of the shear bands.

An extreme fine meshing of the whole workpiece geometry is offered by many FE-simulation software packages. In case of a very high refinement of the whole mesh, which is necessary to model the chip segmentation process, the computational effort strongly

increases. A variation of the influencing parameters and fundamental evaluations to the shear band formation respectively are therefore limited.

For this reason an external remesher, which allows a local refinement in the expected shear zone of the chip, is integrated into the FE-simulations. For this purpose, the user can define „moving boxes“ that allow a concentrated refining of the FE-mesh (Figure 3). The mesher is integrated by a self developed subroutine that also enables a separate definition of meshing parameters and box range. In addition, the cutting speed serves for a coupling of the boxes to the moving tool or a dynamical accommodation of the box range.

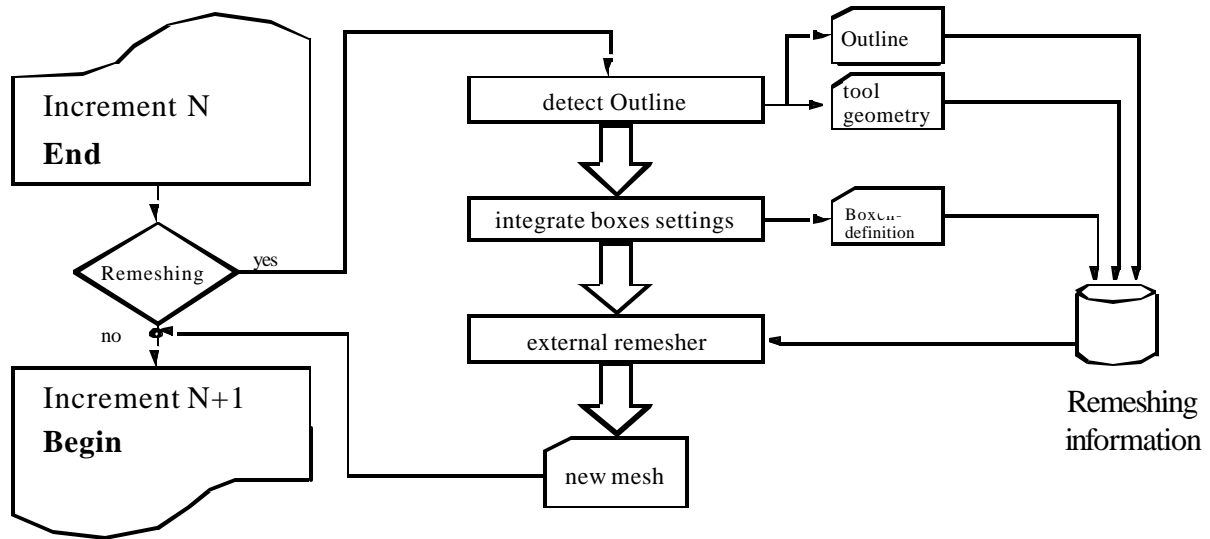


Figure 4 Flow chart for the remeshing technique with moving boxes

If a remeshing is indicated by the FE-program (e.g. in case of mesh distortion), a subroutine determines the outline of the workpiece geometry and the tool geometry. Then a program is invoked that, depending on actual time and cutting speed, calculates the adjacent position of the refining boxes and assigns the current refinement level. As the output file format of the external remesher is coherent to the internal format of MSC.AutoForge, the newly created mesh can be given back for the transfer of the old values to the new mesh to the solver. No manual intervention is necessary as the whole process runs automatically (Figure 4).

4 Material Data and material laws

The realistic modeling of the metal-cutting process implicits the integration of the thermo-mechanical material behavior and the real dynamic material flow of the material. Dynamical stress-strain curves describe the yield stress depending on the deformation strain ϵ , the deformation ratio $\dot{\epsilon}$ and the temperature J .

In the chip formation process, extremely high and localized forming velocities occur, combined with high temperatures and deformation strains. These extreme values cannot simply be referred to uniaxial state of stresses in the determination of the yield stress.

For the description of the dynamic material behavior of Ck 45 N El-Magd et al. Eq. 4. The dependency of the yield stress from the deformation ratio $\dot{\epsilon}$ for low and medium velocities is modeled by a thermally activated slip, and at high strain rates the dominating damping parts have to be taken into consideration [6]. They cause a linear increase of the yield stress proportional to the forming velocity.

$$\text{Eq. 4} \quad s(\dot{\epsilon}, \ddot{\epsilon}, T) = s(\dot{\epsilon}, \ddot{\epsilon}, T_0) \cdot y(T) \quad \text{with} \quad s(\dot{\epsilon}, \ddot{\epsilon}, T_0 = 293 K) = K(B + e^n) + h\dot{\epsilon}$$

The parameters n and h are constant for small temperature intervals, so that the temperature dependance can be implemented with a suitable temperature function $y(T)$. The necessary material parameters of the material Ck 45 N were determined in Split-Hopkinson-Bar tests [6].

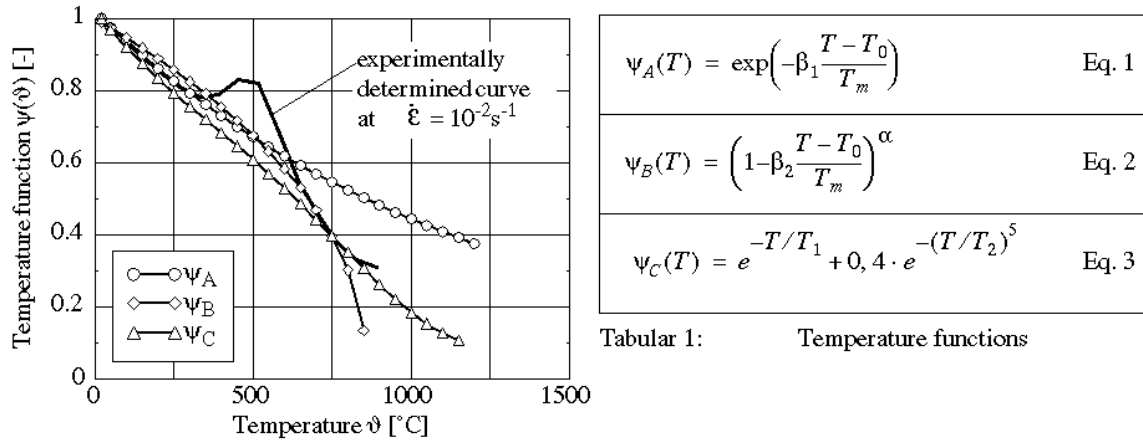


Figure 5 Temperature function of the material Ck 45 N

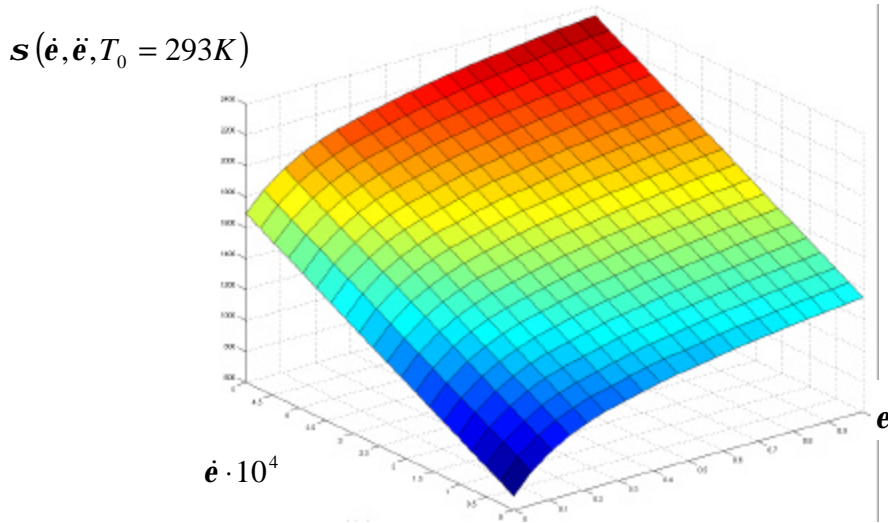


Figure 6 Isothermal yield stress at room temperature

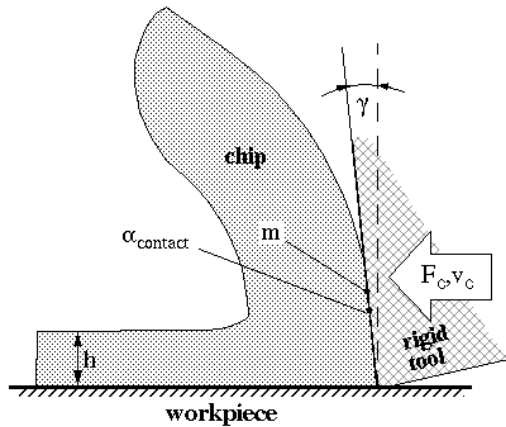
Different empirical equation are suitable for describing the temperature function (Eq. 1 until Eq. 3), all approximating calculated temperatures with real values coming from experiments (mostly at room temperature). The quantitative behavior of the different functions is shown in Figure 5.

In Figure 6 the stress function $s(\dot{\epsilon}, \ddot{\epsilon}, T_0 = 293K)$ from Eq. 4 is shown at room temperature. With growing deformation velocity, the yield stress rises linear, thus increasing the hardening of the material.

5 Simulation of the Orthogonal cutting process

5.1 Model definition

The orthogonal cutting process is characterized by a planar state of stresses perpendicular to the cutting direction. The most relevant parameters for the simulation model (Figure 7) are derived by experimental studies of an orthogonal cutting process, carried out by Friemuth et al.[7]. The cutting conditions were technically realised by turning off a flange of 3 mm width in a plunge-cut process. The feed had an amount of $h=0,1$ mm and a slightly negative cutting angle of $\gamma = -6^\circ$ was chosen. The cutting experiments were carried out without cooling lubricants on the material Ck 45 N; the material of the tool was coated cutting alloy. At a cutting speed of $v_c = 2000$ m/min the cutting force is approximately 800 N.



process	
chip thickness	$h = 0,1 \text{ mm}$
chip width	$b = 3 \text{ mm}$
cutting speed	2000 m/min
workpiece (Ck45 N)	
initial temperature	$\vartheta_{Start} = 20^\circ \text{C}$
E, c_p, λ, ρ	after [8]
yield stress	Eq. 4
tool (HC)	
cutting angle	$\gamma = -6^\circ$
tool model	starrer Körper
contact zone	
heat transmission coefficient	$\alpha_{Kontakt} = 0 \frac{W}{m^2 K}$
shear friction coefficient	$m=0,3$

Figure 7 Modeled cutting process

The lower part of the workpiece volume that does not take part in the chip forming process is implemented as a line segment in the FE-simulations. The tool has the same negative cutting angle of $\phi = -6^\circ$ as in the experiments. The geometrical separation criterion causes the node separation directly in front of the cutting edge. The tool is modeled rigid, neglecting the heat transfer between workpiece, chip and tool because of the short process time. This may result in a slight over- estimation of the calculated temperatures, due to lacking heat transfer in the tool. The dynamic material law from Chap. 4 is used to model the material properties of Ck 45 N. Then the chip forming is a function of the material law function only as no other important parameters for a forced chip formation are given in the model (e.g. a pre-defined fracture as in [1]). From this model, the chip formation can only be initiated by a deformation localization as a consequence of the yield stress function when the softening of material by increasing temperature is higher than the hardening due to deformation and strain.

In order to investigate the exact behavior of the segmentation process, the mesh must be extremely refined in the shear zone. The refining with moving boxes, as described in Chap. 3, is utilized for this purpose. Local increases in temperature and deformation might not be detected in case of an oversized mesh, thus preventing the desired segmentation of the chip. The mesh in the shear zone was discretized to $3\mu\text{m}$ element edge length (Figure 8).



Figure 8 Mesh refining in the shear zone

5.2 Forming of the segmented chip

The slight curvature in the primary shear zone (shear band) of the arising segmented chip of Figure 9(2) points away from the tool. The primary shear zone is known to be the area of maximum strain rate. During the proceeding simulation the curvature changes, thus detaching the first lamella at the end of the segmentation process (Figure 9(5)) as a result of the shear band curvature. The detached lamella touches the workpiece and this self-contact

may lead to an abortion of the simulation. The reason for this is the inability of the remesher to identify a proper outline of the workpiece.

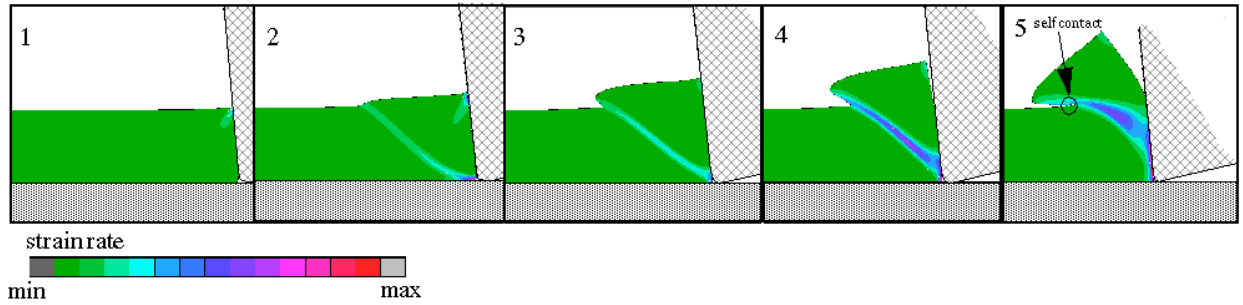


Figure 9 Forming of the first lamellar chip until self contact

The self-contact denoted in Figure 9 (5) of the first lamella refuses further segmentation of the chip. As a consequence, it was necessary to integrate a supporting tool into the model, that moves relatively to the cutting tool with a cutting speed of v_c in a defined distance of x_a from the cutting edge (Figure 10). The formed chip then first comes into contact with the supporting tool instead of the workpiece.

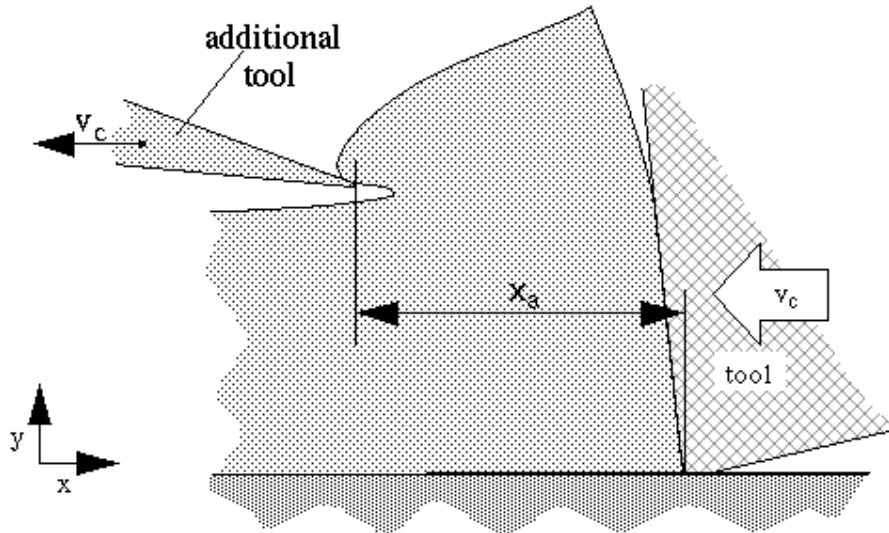


Figure 10 Additional tool for the avoidance of self contact

Now the forming of several segmented chips as shown in Figure 11 can be simulated. The progression of the chips can be identified with the resolution of the mesh. The resolution is identical to the initial FE-mesh and it shows the deformation in case no remeshing occurs. It is clearly visible that the first segment is bigger than the following ones.

material:	Ck45 N
chip width:	$b = 3 \text{ mm}$
chip thickness:	$h = 0,1 \text{ mm}$
cutting speed:	$v_c = 2000 \text{ m/min}$
cutting angle:	$\gamma = -6^\circ$
shear frict. factor:	$m = 0,7$

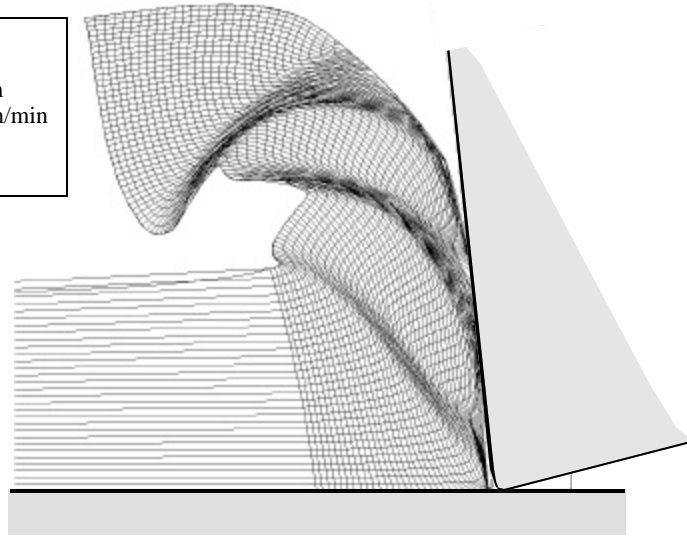


Figure 11 Distribution of shear localization with marker grid

A deformation in the primary shear zone (shear band) can be observed during the chip segmentation process. Figure 12A shows the evolution of the primary shear zone after the forming of the third and before generating the fourth segment. The shear zone progresses from the outside of the chip towards the cutting edge and has a curvature. The end is located above the cutting radius. At the same time, the next shear zone arises starting from the cutting tip. The shear zone, leading to the formation of the fourth segment, has a sigmoid curvature at first (Figure 12B), then it proceeds nearly straightly from the cutting radius to the workpiece surface (Figure 12C) and ends finally into the same sigmoid curvature it had at the beginning (Figure 12D).

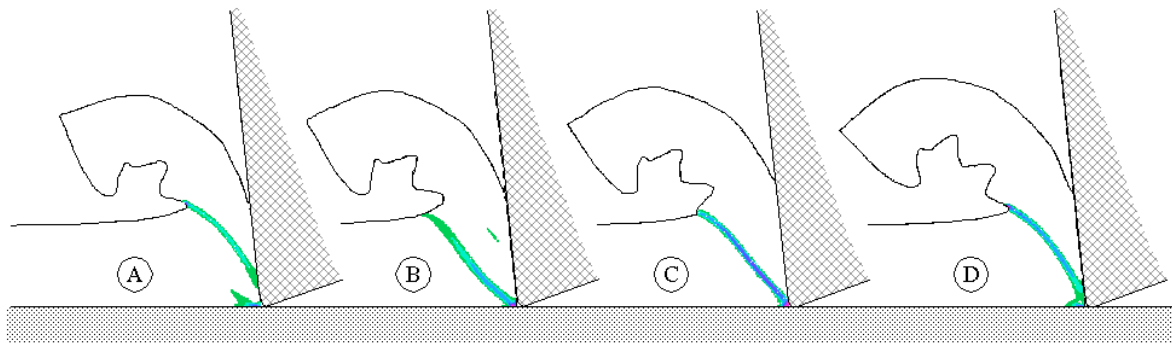


Figure 12 Primary shear zone at the forming of lamellar chips

6 Results

6.1 Temperature distribution in the segmented chip forming process

In Figure 13 the distribution of temperature along the path \overline{AB} is shown for the first lamella. In the middle of the shear band a temperature of approx. 800 °C occurs while the surrounding area reaches less then 200°C only. The temperatures in the contact area between chip and cutting tool are at least as high as in the shear band region, and in some cases they are even higher.

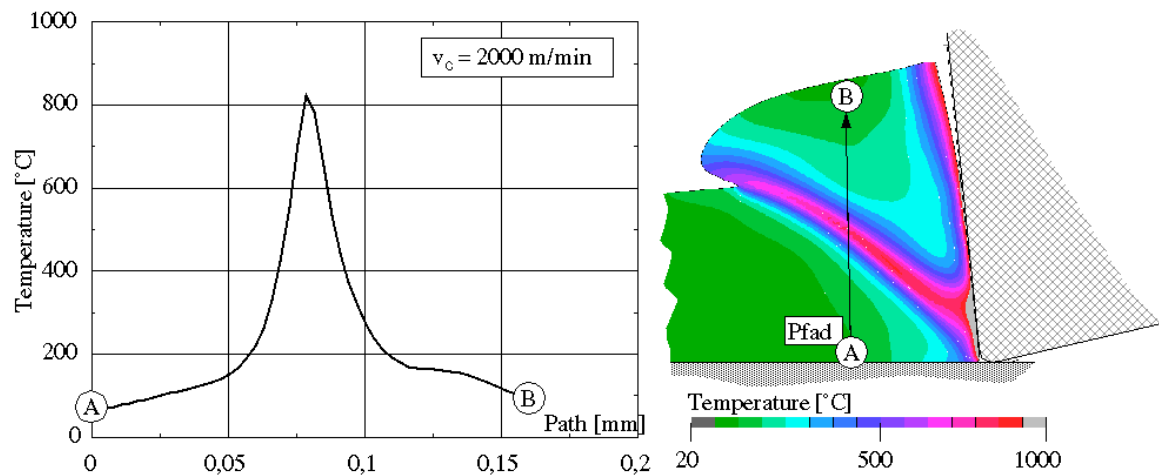


Figure 13 Temperature distribution in the lamella

Figure 14 shows the temperature distribution in the off-running chip and in the chip forming zone after eight segments have been developed.

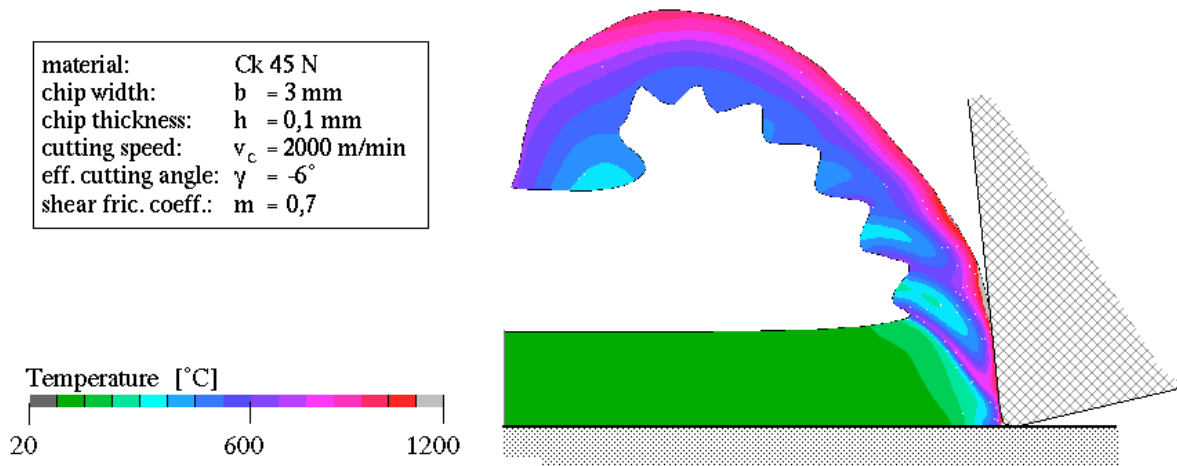


Figure 14 Shear localization and temperature distribution in the segmented chip

6.2 Investigation of the cutting force

For the determination of the cutting force by FE-simulation of the chip forming process it is sufficient to regard a relatively short distance, as a constant force attunes briefly after the first cut. By the use of high coefficients of shear friction ($0,95 \leq m \leq 1$) a slight overshooting of the force occurs in the first cut. This is ascribed to an extreme jump of the material before the cutting edge. After reaching the maximum value, the force decreases to a constant level. In the segmentation process, a maximum force after the first cut attunes the extreme decreases as a consequence of the deformation localization (Figure 15). In the growing shear band, relatively high strain rates, deformations and temperatures occur compared to the surrounding material.

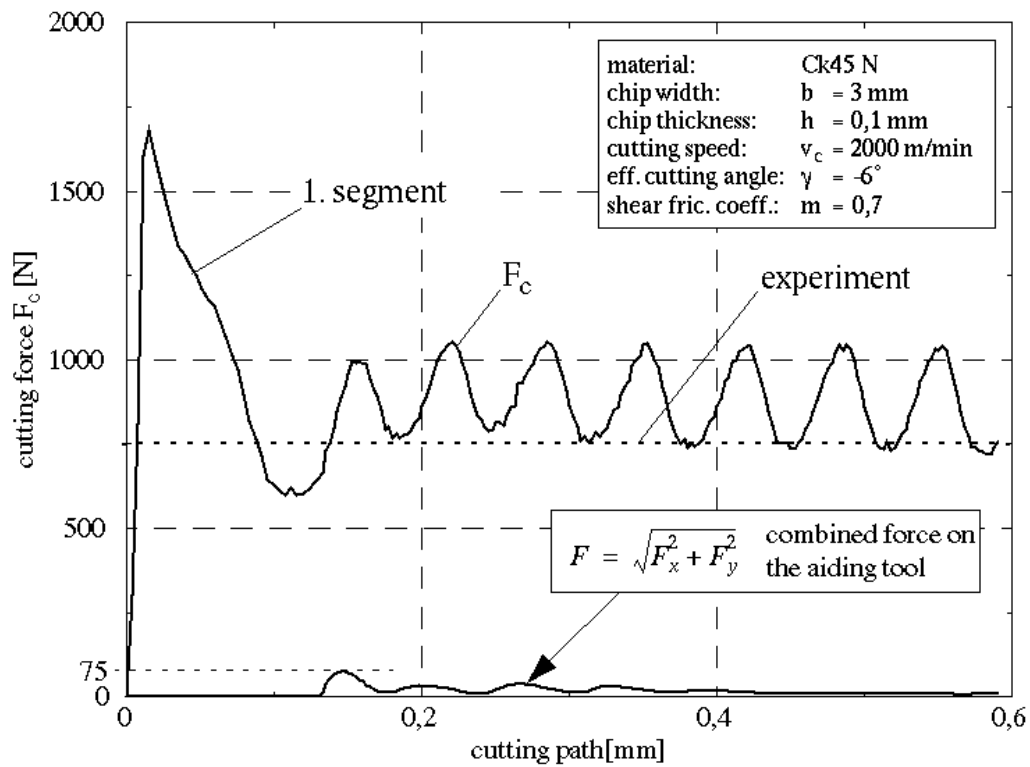


Figure 15 Distribution of the cutting force over the cutting path

Due to the detachment of the lamella in the area of the cutting edge and the adjacent decrease in contact length, the influence of the friction on the FE-simulations fades. Extremely high shear friction coefficients ($m \leq 0,9$) have no significant influence on the calculated contact length or the cutting force during the segmentation of the chip.

The supporting tool's influence on the geometry of the formed chip can also be neglected, as an analysis of the force distribution over the cutting path shows (Figure 15). The dimension of the forces induced by the supporting tool is not relevant compared to the cutting force. A maximum force of 75 N is applied on the supporting tool during the formation of the first

lamella. The force then decreases subsequently and the influence on the chip formation goes back.

The cutting force shown in Figure 15 oscillates with the third chip formation. The cutting force in the first cut is higher due to the larger geometry of the first segment. The dimension of the measured force in the experiment ($v_c=2000\text{m/min}$ in [7]) coincides well with the simulated values.

7 Acknowledgements

The authors wish to thank the Deutsche Forschungsgemeinschaft for the funding of this research project.

8 References

- [1] Bäker, M.; Rösler, J.; Siemers, C.: *Spanbildung bei der Hochgeschwindigkeitszerspanung von Titan-Legierungen.*, Spanen metallischer Werkstoffe mit hohen Geschwindigkeiten, Kolloquium des Schwerpunktprogramms der Deutschen Forschungsgemeinschaft am 18.11.1999 in Bonn
- [2] Bai, Y.; Dodd, B.: *Adiabatic Shear Localization*, Pergamon Press, Oxford, New York, 1992
- [3] Behrens, A.; Westhoff, B.: *Finite Element Modeling of High Speed Machining Processes*, 2nd International German and French Conference on High Speed Machining, 10.-11. März 1999, Darmstadt, S. 185-190
- [4] Childs, T. H. C.: *Material Properties Requirements for Modelling Metal Machining*, Journal de Physique IV, Vol. 7 (1997), S. XXI- XXXVI
- [5] Clos, R.; Schreppel, U.; Veit, P.: *Temperaturentwicklung bei der Ausbildung adiabatische Scherbänder*, Spanen metallischer Werkstoffe mit hohen Geschwindigkeiten, Kolloquium des Schwerpunktprogramms der Deutschen Forschungsgemeinschaft am 18.11.1999 in Bonn
- [6] El-Magd, E.; Treppmann, C.: *Stoffgesetze für hohe Dehngeschwindigkeiten*, Spanen metallischer Werkstoffe mit hohen Geschwindigkeiten, Kolloquium des Schwerpunktprogramms der Deutschen Forschungsgemeinschaft am 18.11.1999 in Bonn
- [7] Friemuth, T.; Andrae, P.; Ben Amor, R.: *High-Speed Cutting - Potential and Demand*, First Saudi Technical Conference & Exhibition, Conference Proceedings Vol. III, Riyadh 18-22 November 2000, S. 210-223
- [8] N.N.: *Stahl-Eisen-Werkstoffblätter (SEW)*, Verein Deutscher Eisenhüttenleute Verlag Stahleisen mbH, Düsseldorf, 1992

- [9] Warnecke, G. *Spanbildung bei metallischen Werkstoffen*, München, Technischer Verlag Resch, 1974